

# A challenge to lepton universality in $B$ -meson decays

Gregory Ciezarek<sup>1</sup>, Manuel Franco Sevilla<sup>2</sup>, Brian Hamilton<sup>3</sup>, Robert Kowalewski<sup>4</sup>, Thomas Kuhr<sup>5</sup>, Vera Lüth<sup>6</sup> & Yutaro Sato<sup>7</sup>

One of the key assumptions of the standard model of particle physics is that the interactions of the charged leptons, namely electrons, muons and taus, differ only because of their different masses. Whereas precision tests comparing processes involving electrons and muons have not revealed any definite violation of this assumption, recent studies of  $B$ -meson decays involving the higher-mass tau lepton have resulted in observations that challenge lepton universality at the level of four standard deviations. A confirmation of these results would point to new particles or interactions, and could have profound implications for our understanding of particle physics.

More than 70 years of particle physics research have led to an elegant and concise theory of particle interactions at the sub-nuclear level, commonly referred to as the standard model<sup>1,2</sup>. On the basis of information extracted from experiments, theorists have combined the theory of electroweak interactions with quantum chromodynamics, the theory of strong interactions, and experiments have validated this theory to an extraordinary degree. Any observation that is proven to be inconsistent with standard model assumptions would suggest a new type of interaction or particle.

In the framework of the standard model of particle physics, the fundamental building blocks, quarks and leptons, are each grouped in three generations of two members each. The three generations of charged leptons—the electron ( $e^-$ ), the muon ( $\mu^-$ ) and the tau ( $\tau^-$ )—are each paired with an electrically neutral lepton, a very low mass neutrino,  $\nu_e$ ,  $\nu_\mu$  and  $\nu_\tau$ , respectively. The electron, a critical component of matter, was discovered by Thomson<sup>3</sup> in 1897. The discovery of the muon in cosmic rays by Anderson and Neddermeyer<sup>4</sup> in 1937 came as a surprise. Similarly surprising was the first observation of  $\tau^+\tau^-$  pair production by Perl *et al.*<sup>5</sup> at the SPEAR  $e^+e^-$  storage ring in 1975. As far as we know, all leptons are point-like particles, that is, they have no substructure.

The three generations are ordered by the mass of the charged lepton, which ranges from 0.511 MeV for  $e^\pm$  to 105 MeV for  $\mu^\pm$  and to 1,777 MeV for  $\tau^\pm$  (ref. 6). These different masses lead to vastly different lifetimes, from the stable electron to 2.2  $\mu$ s for muons, and to 0.29 ps for taus. Charged leptons participate in electromagnetic and weak interactions, but not in strong interactions, whereas neutrinos only undergo weak interactions. The standard model assumes that these interactions of the charged and neutral leptons are universal, that is, the same for the three generations.

Precision tests of lepton universality have been performed over many years by many experiments. To date no definite violation of lepton universality has been observed. Among the most precise tests is a comparison of the decay rates of  $K$  mesons, that is,  $K^- \rightarrow e^- \bar{\nu}_e$  versus  $K^- \rightarrow \mu^- \bar{\nu}_\mu$  (ref. 7). (Unless stated otherwise, the inclusion of charged-conjugate states and decay modes is implied here and in the following.) Furthermore, taking into account precision measurements of the tau and muon masses and lifetimes and the decay rates  $\tau^- \rightarrow e^- \bar{\nu}_e \nu_\tau$  and  $\mu^- \rightarrow e^- \bar{\nu}_e \nu_\mu$ , the equality of the weak coupling strengths of the tau and muon was confirmed<sup>6</sup>. On the other hand, a recent determination of the proton ( $p$ ) radius, derived from very precise measurements of the Lamb shift in muonic hydrogen atoms<sup>8</sup>, differs by about 4% from measurements of normal hydrogen atoms and  $e$ - $p$  scattering data. Studies of the origin of this puzzling

difference are underway<sup>9</sup>. They are aimed at a better understanding of the proton radius and structure, and may reveal details of the true impact of muons and electrons on these interactions.

Recent studies have focused on purely leptonic decays of  $B$  mesons of the form  $B^- \rightarrow \tau^- \bar{\nu}_\tau$  and semileptonic  $B$  decays such as  $\bar{B} \rightarrow D^{(*)} \ell^- \bar{\nu}_\ell$ , with  $\ell = e, \mu$  or  $\tau$ , and where  $D^{(*)}$  refers to a low-mass charm meson,  $D$  or  $D^*$ . These studies have resulted in observations that seem to challenge lepton universality. These weak decays involving leptons are well understood in the framework of the standard model, and therefore offer a unique opportunity to search for unknown phenomena and processes involving new particles: for instance, a yet undiscovered charged partner of the Higgs boson<sup>10</sup>. Such searches have been performed on data collected by three different experiments: the LHCb experiment at the  $pp$  collider at CERN in Europe, and the BaBar and Belle experiments at  $e^+e^-$  colliders in the USA and in Japan, respectively.

Measurements by these three experiments favour larger than expected rates for semileptonic  $B$  decays involving  $\tau$  leptons. Currently, the combined significance of these results is at the level of four standard deviations, and the fact that all three experiments report an unexpected enhancement has drawn considerable attention. A confirmation of this violation of lepton universality and an explanation in terms of new-physics processes would be very exciting. In the following, we present details of the experimental techniques and preliminary studies to understand the observed effects, along with prospects of improved sensitivity and complementary measurements at current and future facilities.

## Standard model predictions of $B$ -meson decay rates

According to the standard model, purely leptonic and semileptonic decays of  $B$  mesons are mediated by the  $W^-$  boson, as shown schematically in Fig. 1.  $B$  mesons are assumed to be composed of a  $b$ -quark and an antiquark (anti- $u$  or anti- $d$ ), either  $B^-(b, \bar{u})$  or  $\bar{B}^0(b, \bar{d})$ , whereas charm mesons (the spin-0  $D$  and spin-1  $D^*$  state) contain a  $c$ -quark and an antiquark (anti- $u$  or anti- $d$ ),  $D^{0(*)}(c, \bar{u})$  or  $D^{+(*)}(c, \bar{d})$ .

For purely leptonic  $B^-$  decays, the standard model prediction of the total decay rate  $\Gamma$ , which depends critically on the lepton mass squared  $m_\ell^2$ , is:

$$\Gamma^{\text{SM}}(B^- \rightarrow \ell^- \bar{\nu}_\ell) = \frac{G_F^2 m_B m_\ell^2}{8\pi} |V_{ub}|^2 \left(1 - \frac{m_\ell^2}{m_B^2}\right)^2 f_B^2 \quad (1)$$

<sup>1</sup>Nikhef National Institute for Subatomic Physics, Amsterdam, The Netherlands. <sup>2</sup>University of California at Santa Barbara, Santa Barbara, California 93106, USA. <sup>3</sup>University of Maryland, College Park, Maryland 20742, USA. <sup>4</sup>University of Victoria, Victoria, British Columbia V8P 5C2, Canada. <sup>5</sup>Ludwig Maximilians University, 80539 Munich, Germany. <sup>6</sup>SLAC National Accelerator Laboratory, Stanford, California 94309, USA. <sup>7</sup>Kobayashi-Maskawa Institute, Nagoya University, Nagoya 464-8602, Japan.

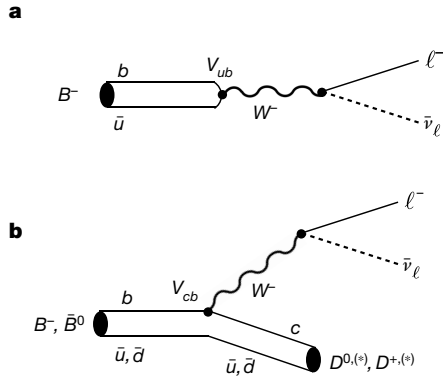


**Figure 1 | Diagrams for standard-model decay processes. a,  $B^- \rightarrow \ell^- \bar{\nu}_\ell$ , with a purely leptonic final state. b,  $\bar{B} \rightarrow D^{(*)} \ell^- \bar{\nu}_\ell$ , involving a charm meson ( $D$  or  $D^*$ ) and lepton pair and mediated by a vector boson ( $W^-$ ).  $V_{ub}$  and  $V_{cb}$  refer to the quark mixing parameters in  $b \rightarrow u$  and  $b \rightarrow c$  transitions (commonly referred to as CKM parameters<sup>13</sup>).**

The first factor contains the Fermi constant  $G_F = 1.1663797 \times 10^{-5} \text{ GeV}^{-2}$  and the  $B$ -meson mass,  $m_B = 5.279 \text{ GeV}$ . All hadronic effects, due to the binding of quarks inside the meson, are encapsulated in the decay constant  $f_B$ . Recent lattice quantum chromodynamics calculations<sup>11</sup> predict  $f_B = (0.191 \pm 0.009) \text{ GeV}$ . Taking into account the current world averages for the  $B^-$  lifetime,  $\tau_B = (1.638 \pm 0.004) \text{ ps}$  (ref. 12), and the quark mixing parameter<sup>13</sup> for  $b \rightarrow u$  transitions,  $|V_{ub}|$  (ref. 14), the expected branching fraction, that is, the frequency of this decay relative to all decay modes, is (ref. 15, and recent updates at <http://ckmfitter.in2p3.fr>):

$$\mathcal{B}^{\text{SM}}(B^- \rightarrow \tau^- \bar{\nu}_\tau) = (0.75 \pm_{0.05}^{0.10}) \times 10^{-4} \quad (2)$$

Decays to the lower-mass charged leptons,  $e^-$  and  $\mu^-$ , are strongly suppressed by spin effects and have not yet been observed.

The differential decay rate,  $d\Gamma$ , for semileptonic decays involving  $D^{(*)}$  mesons depends on both  $m_\ell^2$  and  $q^2$ , the invariant mass squared of the lepton pair<sup>16</sup>:

$$\frac{d\Gamma^{\text{SM}}(\bar{B} \rightarrow D^{(*)} \ell^- \bar{\nu}_\ell)}{dq^2} = \frac{G_F^2 |V_{cb}|^2 |p_{D^{(*)}}^*|^2 q^2 \left(1 - \frac{m_\ell^2}{q^2}\right)^2}{96\pi^3 m_B^2} \underbrace{\left[ (|H_+|^2 + |H_-|^2 + |H_0|^2) \left(1 + \frac{m_\ell^2}{2q^2}\right) + \frac{3m_\ell^2}{2q^2} |H_s|^2 \right]}_{\text{Hadronic effects}} \quad (3)$$

The first factor is universal for all semileptonic  $B$  decays, containing a quark flavour mixing parameter<sup>13</sup>, in this case  $|V_{cb}|$  (ref. 14) for  $b \rightarrow c$  quark transitions, and  $p_{D^{(*)}}^*$ , the 3-momentum of the hadron in the  $B$  rest frame, in this case a  $D$  or  $D^*$  meson. The four helicity amplitudes  $H_+$ ,  $H_-$ ,  $H_0$  and  $H_s$  capture the impact of hadronic effects. (Helicity refers to the component of the angular momentum of a particle parallel to the direction of its momentum.) They depend on the spin of the charm meson and on  $q^2$ . The kinematic range,  $m_\ell^2 \leq q^2 \leq (m_B - m_{D^{(*)}})^2$ , is sensitive to the lepton mass  $m_\ell$  and the charm meson mass  $m_{D^*}$ . The much larger mass of the  $\tau$  not only affects the rate, but also the kinematics of the decays via the  $H_s$  amplitude. All four amplitudes contribute to  $\bar{B} \rightarrow D^* \ell^- \bar{\nu}_\ell$ , while only  $H_0$  and  $H_s$  contribute to  $\bar{B} \rightarrow D \ell^- \bar{\nu}_\ell$ , which leads to a higher sensitivity of this decay mode to the scalar contribution  $H_s$ .

Measurements of the ratios of semileptonic branching fractions remove the dependence on  $|V_{cb}|$ , lead to a partial cancellation of theoretical uncertainties related to hadronic effects, and reduce the impact of experimental uncertainties. Current standard model predictions<sup>17–19</sup> are:

$$\mathcal{R}_D^{\text{SM}} = \frac{\mathcal{B}(\bar{B} \rightarrow D \tau^- \bar{\nu}_\tau)}{\mathcal{B}(\bar{B} \rightarrow D e^- \bar{\nu}_e)} = 0.300 \pm 0.008 \quad (4)$$

$$\mathcal{R}_{D^*}^{\text{SM}} = \frac{\mathcal{B}(\bar{B} \rightarrow D^* \tau^- \bar{\nu}_\tau)}{\mathcal{B}(\bar{B} \rightarrow D^* e^- \bar{\nu}_e)} = 0.252 \pm 0.003 \quad (5)$$

The predicted ratios relative to  $\mathcal{B}(\bar{B} \rightarrow D^* \mu^- \bar{\nu}_\mu)$  are identical within the quoted precision.

## B-meson production and detection

$B$ -meson decays have been studied at  $pp$  and  $e^+e^-$  colliding beam facilities operating at very different beam energies. The  $e^+e^-$  colliders operated at a fixed energy of 10.579 GeV in the years 1999 to 2010. At this energy, about 20 MeV above the kinematic threshold for  $B\bar{B}$  production,  $e^+$  and  $e^-$  annihilate and produce a particle, commonly referred to as  $\Upsilon(4S)$ , which decays almost exclusively to  $B^+B^-$  or  $B^0\bar{B}^0$  pairs. The maximum production rate for these  $\Upsilon(4S) \rightarrow B\bar{B}$  events of 20 Hz was achieved at KEK (the High Energy Accelerator Research Organization in Tsukuba, Japan), compared to the multi-hadron non- $B\bar{B}$  background rate of about 80 Hz.

$B$  mesons from  $\Upsilon(4S)$  decays have very low momenta, about 300 MeV, and therefore their decay products are distributed almost isotropically in the rest frame of the  $\Upsilon(4S)$ . For this reason, the BaBar<sup>20,21</sup> and Belle<sup>22</sup> detectors were designed to cover close to 90% of the total solid angle, thereby enabling the reconstruction of all final state particles from decays of the two  $B$  mesons, except for neutrinos. Both detectors consist of cylindrical layers of sensors surrounding the beam pipe, plus endcaps to cover the small polar angles. Constraints from energy-momentum conservation allow events containing a single neutrino to be discriminated from those containing multiple undetected particles. This feature also allows for an effective suppression of non- $B\bar{B}$  background and misreconstructed events.

The LHC  $pp$  collider operated at total energies of 7 TeV and 8 TeV from 2008 to 2012. In inelastic  $pp$  collisions, high-energy gluons, the carriers of the strong force between the quarks inside the protons, collide and produce a pair of  $B$  hadrons (mesons or baryons) along with a large number of other charged and neutral particles, in roughly one of every hundred  $pp$  interactions. The  $B$  hadrons are typically produced at small angles to the beam and with high momenta. These features determined the design of the LHCb detector<sup>23,24</sup>, a single-arm forward spectrometer, covering the polar angle range of  $3^\circ$ – $23^\circ$ . The high momentum and relatively long  $B$  hadron lifetime result in decay distances of several centimetres. Very precise measurements of the  $pp$  interaction point, combined with the detection of charged particle trajectories from  $B$  decays which do not intersect this point, are the very effective, primary method to separate  $B$  decays from background.

All three experiments rely on several layers of finely segmented silicon strip detectors to locate the beam–beam interaction point and decay vertices of long-lived particles. A combination of silicon strip detectors and multiple layers of gaseous detectors measure the trajectories of charged particles, and determine their momenta from the deflection in a magnetic field. Examples of reconstructed signal events recorded by the LHCb and Belle experiments are shown in Fig. 2.

For a given momentum, charged particles of different masses, primarily pions and kaons, are identified by their different velocities. All three experiments make use of devices that sense Cherenkov radiation, which is emitted by particles with velocities that exceed the speed of light in a chosen radiator material. For lower-velocity particles, Belle complements this with time-of-flight measurements. BaBar and Belle also measure the velocity-dependent energy loss due to ionization in the tracking detectors. Arrays of caesium iodide crystals measure the energy of photons and identify electrons in BaBar and Belle. Muons are identified as particles penetrating a stack of steel absorbers interleaved with large area gaseous detectors.

## Measurements of $B^- \rightarrow \tau^- \bar{\nu}_\tau$ decays

The decays  $B^- \rightarrow \tau^- \bar{\nu}_\tau$  with two or three neutrinos in the final state have only been observed by the BaBar and Belle collaborations. These two experiments exploit the  $B\bar{B}$  pair production at the  $\Upsilon(4S)$  resonance via

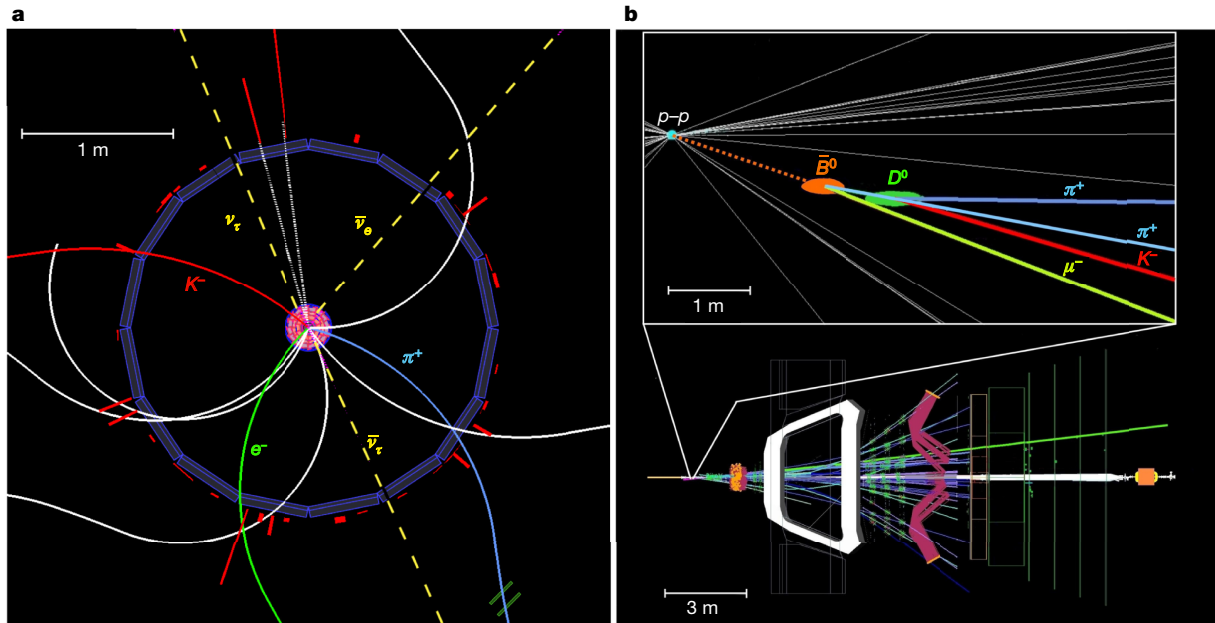


**Figure 2 | Belle and LHCb single-event displays illustrating the reconstruction of semileptonic  $B$ -meson decays.** Trajectories of charged particles are shown as coloured solid lines; energy deposits in the calorimeters are depicted by red bars. **a**, The Belle display is an end view perpendicular to the beam axis, with the silicon detector in the centre (small orange circle) and the device measuring the particle velocity (dark purple polygon). This is a  $\Upsilon(4S) \rightarrow B^+B^-$  event, with  $B^- \rightarrow D^0\tau^-\bar{\nu}_\tau$ ,  $D^0 \rightarrow K^-\pi^+$  and  $\tau^- \rightarrow e^-\nu_e\bar{\nu}_\tau$ , and the  $B^+$  decaying to five charged particles (white solid lines) and two photons. The trajectories of undetected

neutrinos are marked as dashed yellow lines. **b**, The LHCb display is a side view, with the proton beams indicated as a white horizontal line with the interaction point far to the left, followed by the dipole magnet (white trapezoid) and the Cherenkov detector (red lines). The area close to the interaction point is enlarged above, showing the tracks of the charged particles produced in the  $pp$  interaction, the  $B^0$  path (dotted orange line), and its decay  $B^0 \rightarrow D^{*+}\tau^-\bar{\nu}_\tau$ , with  $D^{*+} \rightarrow D^0\pi^+$  and  $D^0 \rightarrow K^-\pi^+$ , plus the  $\mu^-$  from the decay of a very short-lived  $\tau^-$ .

the process  $e^+e^- \rightarrow \Upsilon(4S) \rightarrow B\bar{B}$ . These  $B\bar{B}$  pairs can be tagged by the reconstruction of a hadronic or semileptonic decay of one of the two  $B$  mesons, referred to as  $B_{\text{tag}}$ . If this decay is correctly reconstructed, all remaining particles in the event originate from the other  $B$  decay, either a signal leptonic or semileptonic  $B$  decay or another  $B$  decay passing the selection criteria.

The BaBar and Belle collaborations have independently developed two sets of algorithms to tag  $B\bar{B}$  events. The hadronic tag algorithms<sup>25,26</sup> search for the best match between one of more than a thousand possible decay chains and a subset of all detected particles in the event. The efficiency for finding a correctly matched  $B_{\text{tag}}$  is unfortunately quite small, 0.3%. The benefit of reconstructing all final state particles is that the total energy,  $E_{\text{miss}}$ , and momentum vector,  $\mathbf{p}_{\text{miss}}$ , of all undetected particles of the other  $B$  decay can be inferred from energy and momentum conservation. The invariant mass squared of all undetected particles,  $m_{\text{miss}}^2 = E_{\text{miss}}^2 - \mathbf{p}_{\text{miss}}^2$ , is used to distinguish events with one neutrino ( $m_{\text{miss}}^2 \approx 0$ ) from events with multiple neutrinos or other missing particles ( $m_{\text{miss}}^2 > 0$ ). The semileptonic tag algorithms exploit the large branching fractions for  $B$  decays involving a charm meson, a charged lepton and associated neutrino,  $B \rightarrow D^{(*)}\ell^+\nu_\ell$ , with  $\ell^+ = e^+, \mu^+$ . The efficiency for finding these tag decays is about 1%. However, the presence of the neutrino leads to weaker constraints on the  $B_{\text{tag}}$  and signal  $B$  decay.

Measurements of  $B^- \rightarrow \tau^-\bar{\nu}_\tau$  decays are based on leptonic  $\tau$  decays,  $\tau^- \rightarrow e^-\bar{\nu}_e\nu_\tau$  and  $\tau^- \rightarrow \mu^-\bar{\nu}_\mu\nu_\tau$ , and on semileptonic  $\tau$  decays,  $\tau^- \rightarrow \pi^-\nu_\tau$  and  $\tau^- \rightarrow \pi^-\pi^0\nu_\tau$ , which together account for 70% of all  $\tau^-$  decays. Thus, the signature for signal events is a single charged particle, either a charged lepton, a  $\pi^-$ , or a  $\pi^-$  accompanied by a  $\pi^0$ , plus a  $B_{\text{tag}}$ .

The presence of multiple neutrinos precludes the use of kinematic constraints to effectively suppress backgrounds from other  $B$  decays. A variable that is sensitive to backgrounds with additional photons or undetected charged particles due to efficiency and acceptance losses is  $E_{\text{extra}}$ , the sum of the energy deposits in the calorimeter which are not associated with the tag or signal  $B$  decay. Figure 3 shows a  $E_{\text{extra}}$  distribution measured by the Belle collaboration for a subset of events with

$\tau^- \rightarrow \pi^-\nu_\tau$ . Signal events have low values of  $E_{\text{extra}}$ , while background events extend to higher values. The signal yield is determined from a fit to the data using signal and background distributions based on data control samples and Monte Carlo simulation. The sum of the fitted signal yields for the four subsamples of purely leptonic and semileptonic  $\tau$  decays, corrected for the efficiency of the tag and signal  $B$  decays, is used to determine the  $B^- \rightarrow \tau^-\bar{\nu}_\tau$  branching fraction.

As shown in Fig. 4, current measurements by the Belle<sup>27,28</sup> and BaBar<sup>29,30</sup> collaborations are of limited precision owing to very small signal samples and high backgrounds, and uncertainties in the  $B_{\text{tag}}$

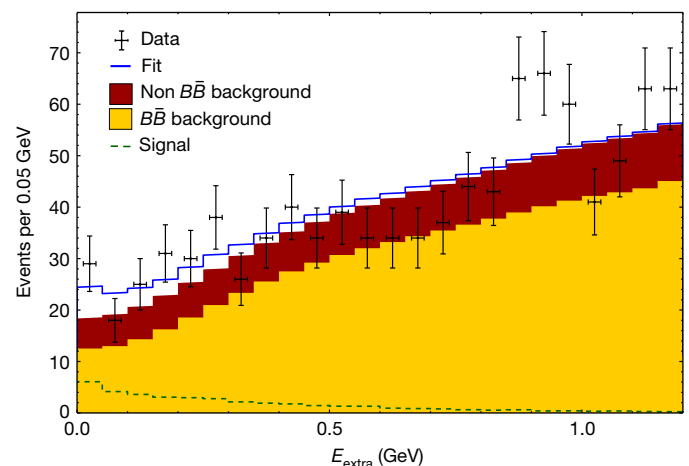


**Figure 3 | Extraction of the  $B^- \rightarrow \tau^-\bar{\nu}_\tau$  yield from Belle data.** Shown, for a subset of events with  $\tau^- \rightarrow \pi^-\nu_\tau$  candidates (solid histogram), is the result of a fit to the  $E_{\text{extra}}$  distribution (data points with statistical errors) for the sum of signal and backgrounds from  $B\bar{B}$  and non- $B\bar{B}$  events<sup>27</sup>. The green histogram at the bottom indicates the predicted signal distribution. Image adapted from ref. 27, American Physical Society.

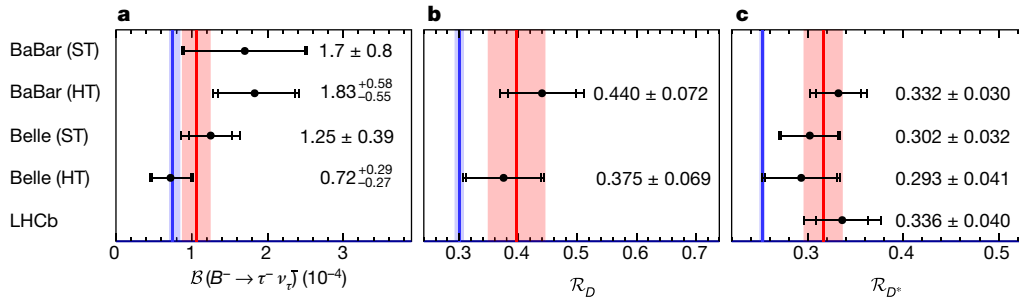


**Figure 4 | Comparison of measurements with standard model predictions.** a–c, Shown are the branching fraction  $\mathcal{B}(B^- \rightarrow \tau^- \bar{\nu}_\tau)$  (a), and the ratios  $\mathcal{R}_D$  (b) and  $\mathcal{R}_{D^*}$  (c) measured by the BaBar<sup>26,29,30</sup>, Belle<sup>27,28,32,33</sup> and LHCb<sup>34</sup> collaborations. The data points indicate statistical and total uncertainties. ST and HT refer to the measurements with semileptonic and

hadronic tags, respectively. The average values of the measurements and their combined uncertainties, obtained by the Heavy Flavor Averaging Group<sup>31,39</sup>, are shown in red as vertical lines and bands, and the expectations from the standard model calculations<sup>15,17,18</sup> are shown in blue.

efficiencies. The combination of these four measurements constitutes the first observation of a purely leptonic  $B^-$  decay. Whereas the early measurements favoured somewhat larger values, the current average<sup>31</sup> of

$$\mathcal{B}(B^- \rightarrow \tau^- \bar{\nu}_\tau) = (1.06 \pm 0.19) \times 10^{-4} \quad (6)$$

is compatible with the standard model prediction (equation (1)), which is lower by 1.4 standard deviations.

### Measurements of $\bar{B} \rightarrow D^{(*)} \tau^- \bar{\nu}_\tau$ decays

As defined in equations (4) and (5),  $\mathcal{R}_{D^{(*)}}$  corresponds to the ratio of branching fractions for  $\bar{B} \rightarrow D^{(*)} \tau^- \bar{\nu}_\tau$  (signal) and  $\bar{B} \rightarrow D^{(*)} \ell^- \bar{\nu}_\tau$  (normalization). BaBar and Belle events containing such decays are selected by requiring a hadronic  $B_{\text{tag}}$ , a  $D$  or  $D^*$  meson, and a charged lepton  $\ell^- = e^-, \mu^-$ . Charged and neutral  $D$  candidates are reconstructed from combinations of pions and kaons with invariant masses compatible with the  $D$  meson mass. The higher-mass  $D^{*0}$  and  $D^{*+}$  mesons are identified by their  $D^* \rightarrow D\pi$  and  $D^* \rightarrow D\gamma$  decays. In signal decays, the lepton  $\ell^-$  originates from the  $\tau^- \rightarrow \ell^- \bar{\nu}_\ell \nu_\tau$  decay, leading to a final state with three neutrinos and resulting in a broad  $m_{\text{miss}}^2$  distribution, while in normalization decays the lepton originates from the  $B$  decay with a single neutrino and therefore  $m_{\text{miss}}^2 \approx 0$ . Non- $B\bar{B}$  backgrounds and misreconstructed events are greatly suppressed by the  $B_{\text{tag}}$  reconstruction. The remaining background is further reduced by multivariate selections.

At LHCb, only decays of  $\bar{B}^0$  mesons producing a  $\mu^-$  and  $D^{*+}$  meson are selected. Muons are favoured over electrons because of their higher detection efficiency and momentum resolution. The  $D^{*+}$  meson is reconstructed exclusively in  $D^{*+} \rightarrow D^0(\rightarrow K^- \pi^+) \pi^+$  decays.  $B$  mesons produced at LHCb have a flight path of the order of 1 cm. This feature is exploited to reject the bulk of the background, by requiring that the charged particles from the  $B$  candidate and no other tracks originate from a common vertex that is significantly separated from the  $pp$  collision point. The reduction in signal efficiency due to the use of a single decay chain is compensated by the very large production rate of  $B$  mesons at the LHC. The direction of the  $B$  momentum is inferred from the reconstructed  $pp$  collision point and the  $D^{*+} \mu^-$  vertex, but its magnitude is unknown. LHCb approximates the  $B$  momentum by equating its component parallel to the beam axis to that of the  $D^{*+} \mu^-$  combination, rescaled by the ratio of the  $B$  mass to the measured  $D^{*+} \mu^-$  mass.

The yields for the signal, normalization, and various background contributions are determined by maximum likelihood fits to the observed data distributions. Control samples are used to validate the simulated distributions and constrain the size and kinematic features of the background contributions.

All three experiments rely on the variables  $m_{\text{miss}}^2$ ,  $E_\ell^*$  (the energy of the charged lepton in the  $B$  rest frame) and  $q^2$ . BaBar and Belle restrict the data to  $q^2 > 4 \text{ GeV}^2$  to enhance the contribution from signal decays. BaBar performs the fit in two dimensions whereas LHCb covers the whole  $q^2$  range in four intervals, thus performing a fully three-dimensional fit. The

Belle collaboration performs a one-dimensional fit to the  $m_{\text{miss}}^2$  distribution in the low- $m_{\text{miss}}^2$  region ( $m_{\text{miss}}^2 < 0.85 \text{ GeV}^2$ ) dominated by the normalization decays, combined with a fit to a multivariate classifier in the high- $m_{\text{miss}}^2$  region. This classifier includes  $m_{\text{miss}}^2$ ,  $E_\ell^*$ ,  $E_{\text{extra}}$ , and additional kinematic variables.

Figure 5 shows one-dimensional projections of the data and the fitted contributions from signal, normalization, and background decays. For BaBar (and likewise for Belle), the  $m_{\text{miss}}^2$  distributions show a narrow peak at zero (Fig. 5a, d), dominated by normalization decays with a single neutrino, whereas the signal events with three neutrinos extend to about  $10 \text{ GeV}^2$ . For  $\bar{B} \rightarrow D \ell^- \bar{\nu}_\tau$  decays, there is a sizeable contribution from  $\bar{B} \rightarrow D^* \ell^- \bar{\nu}_\tau$  decays, for which the pion or photon from the  $D^* \rightarrow D\pi$  or  $D^* \rightarrow D\gamma$  decay was not reconstructed. For LHCb, the peak at zero is somewhat broader and has a long tail into the signal region (Fig. 5h) because of the sizeable uncertainty in the estimation of the  $B_{\text{sig}}$  momentum. The  $E_\ell^*$  distributions (Fig. 5c, f, i) provide additional discrimination, since a lepton from a normalization decay has a higher average momentum than a lepton originating from a secondary  $\tau^- \rightarrow \ell^- \bar{\nu}_\ell \nu_\tau$  decay in signal  $B$  decays.

Among the background contributions, semileptonic  $B$  decays to  $D^{**}$  mesons (charm mesons of higher mass than the  $D^*$  mesons) are of concern, primarily because their branching fractions are not well known. These  $D^{**}$  states decay to a  $D$  or  $D^*$  meson plus additional particles that, if not reconstructed, contribute to the missing momentum of the decay. As a result,  $\bar{B} \rightarrow D^{**} \ell^- \bar{\nu}_\ell$  decays have a broader  $m_{\text{miss}}^2$  distribution than do normalization decays. They can be distinguished from signal decays by their  $E_\ell^*$  distributions which extend to higher values. At LHCb, an important background arises from  $B \rightarrow D^{(*)} H_c X$  decays, where  $H_c$  is a charm hadron decaying either leptonically or semileptonically, and  $X$  refers to additional low-mass hadrons, if present. These decays produce  $m_{\text{miss}}^2$  and  $E_\ell^*$  spectra that are similar to those of signal events (Fig. 5h, i).

Figure 4 shows the measured values for  $\mathcal{R}_D$  and  $\mathcal{R}_{D^*}$  by the BaBar<sup>26</sup>, Belle<sup>32,33</sup> and LHCb<sup>34</sup> collaborations. These results include a recent measurement of  $\mathcal{R}_{D^*}$  by Belle that uses a semileptonic tag, but do not include earlier results from BaBar<sup>35,36</sup> and Belle<sup>37,38</sup> based on partial datasets. The averages of the measurements<sup>39</sup> are

$$\mathcal{R}_D = 0.397 \pm 0.040_{\text{stat}} \pm 0.028_{\text{sys}} \quad (7)$$

$$\mathcal{R}_{D^*} = 0.316 \pm 0.016_{\text{stat}} \pm 0.010_{\text{sys}} \quad (8)$$

Both values exceed the standard model expectations. Taking into account the correlations (Fig. 6), the combined difference between the measured and expected values has a significance of about four standard deviations.

### Interpretations of results

The results presented here have attracted the attention of the physics community, and have resulted in several potential explanations of this apparent violation of lepton universality for decays involving the  $\tau$  lepton.

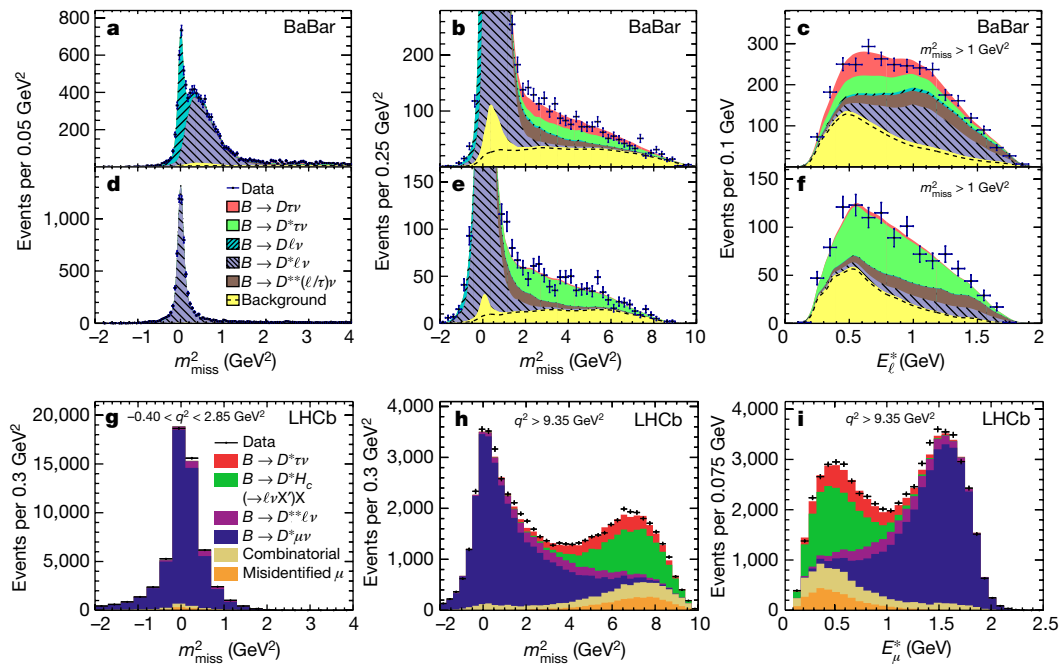


**Figure 5 | Extraction of the ratios  $\mathcal{R}_D$  and  $\mathcal{R}_{D^*}$  by maximum likelihood fits.** Shown are comparisons of the projections of the measured  $m_{\text{miss}}^2$  and  $E_{\ell}^*$  distributions (data points with statistical errors) and the fitted distributions of signal and background contributions (coloured areas; see keys in **d** and **g**) for the fit by the BaBar collaboration<sup>26</sup> to the  $D\ell$  samples (**a–c**) and to the  $D^*\ell$  samples (**d–f**), as well as the fit by the LHCb collaboration<sup>34</sup> to the  $D^{*+}\ell$  sample (**g–i**). The  $D\ell$  samples in **a–c** show sizeable contributions from  $B^0 \rightarrow D^{*+}\ell^-\bar{\nu}_\ell$  and  $B^0 \rightarrow D^{*+}\tau^-\bar{\nu}_\tau$  decays, because the low-energy pion or photon originating from a  $D^* \rightarrow D\pi$  or

$D^* \rightarrow D\gamma$  decay was undetected. The BaBar data exclude  $q^2 < 4 \text{ GeV}^2$ , where the contributions from signal decays is very small. The  $E_{\ell}^*$  distributions in **c** and **f** are signal enhanced by the restriction  $m_{\text{miss}}^2 > 1 \text{ GeV}^2$ . The LHCb results are presented for two different  $q^2$  intervals: the lowest, which is free of  $B^0 \rightarrow D^{*+}\tau^-\bar{\nu}_\tau$  decays (**g**); and the highest, where this contribution is large (**h**, **i**). Panels **a–f** adapted from ref. 26, American Physical Society; panels **g–i** adapted from ref. 34, American Physical Society.

In the standard model, these  $B$  decays are mediated by a virtual charged vector boson, a particle of spin 1, usually referred to as the  $W^-$  (as indicated in the diagram in Fig. 1), which couples equally to all leptons. If a hitherto unknown virtual particle existed that interacted differently with leptons of higher mass such as the  $\tau$ , this could change the  $B$  decay rates and their kinematics.

Among the simplest explanations for the observed rate increases for decays involving  $\tau^-$  would be the existence of a new vector boson,  $W'^-$ ,

similar to the standard model  $W^-$  boson, but with a greater mass, and with couplings of varying strengths to different leptons and quarks. This could lead to changes in  $\mathcal{R}_D$  and  $\mathcal{R}_{D^*}$ , but not in the kinematics of the decays, which are observed to be consistent with the standard model. However, this choice is constrained by searches for  $W'^- \rightarrow \bar{t}b$  decays<sup>40,41</sup> at the LHC collider at CERN, as well as by precision measurements of  $\mu$  (ref. 42) and  $\tau$  (ref. 43) decays.

Another potentially interesting candidate would be a new type of Higgs boson, a particle of spin 0, similar to the recently discovered neutral Higgs<sup>44,45</sup>, but electrically charged. This charged Higgs ( $H^-$ ) was proposed in minimal extensions of the standard model<sup>46</sup>, which are part of broader theoretical frameworks such as supersymmetry<sup>47</sup>. The  $H^-$  would mediate weak decays, similar to the  $W^-$  (as indicated in Fig. 1), but couple differently to leptons of different mass. The  $q^2$  and angular distributions would be affected by this kind of mediator because of its different spin.

Another feasible solution might be leptoquarks<sup>48</sup>, hypothetical particles with both electric and colour (strong) charges that allow transitions from quarks to leptons and vice versa, and offer a unified description of three generations of quarks and leptons. Among the ten different types of leptoquarks, six could contribute to  $B \rightarrow D^{(*)}\tau\nu$  decays<sup>49</sup>. A diagram of a spin-0 state mediating quark-lepton transitions is shown in Fig. 7 for the  $B$  decay modes under study.

The BaBar and Belle collaborations have studied the implications of these hypothetical particles in the context of specific models<sup>26,32</sup>. The measured values of  $\mathcal{R}_D$  and  $\mathcal{R}_{D^*}$  do not support the simplest of the two-Higgs doublet models (type II), however, more general Higgs models with appropriate parameter choices can accommodate these values<sup>50–52</sup>. Some of the leptoquark models could also explain the measured values of  $\mathcal{R}_D$  and  $\mathcal{R}_{D^*}$  (refs 53–55), evading constraints from direct searches of leptoquarks in  $ep$  collisions<sup>56</sup> at HERA<sup>57,58</sup> and  $pp$  collisions at LHC<sup>59,60</sup>.

The three-body kinematics of  $B \rightarrow D^{(*)}\tau\nu$  decays should permit further discrimination of new-physics scenarios based on the decay distributions of final state particles. The  $q^2$  spectrum<sup>26,32</sup> and the momentum

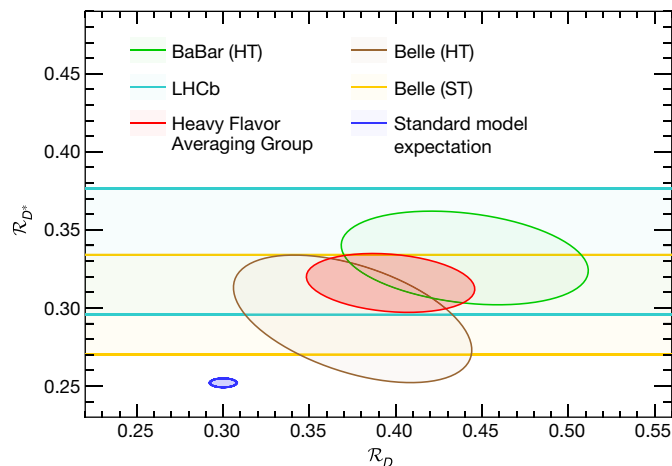


**Figure 6 |  $\mathcal{R}_D$  and  $\mathcal{R}_{D^*}$  measurements.** Results from the BaBar<sup>26</sup>, Belle<sup>32,33</sup> and LHCb<sup>34</sup> collaborations, showing their measured values and  $1\sigma$  contours. The average calculated by the Heavy Flavor Averaging Group<sup>39</sup> (taking into account the statistical and systematic uncertainties and their correlations) is compared to standard model predictions<sup>17–19</sup>. ST and HT refer to the measurements with semileptonic and hadronic tags, respectively.

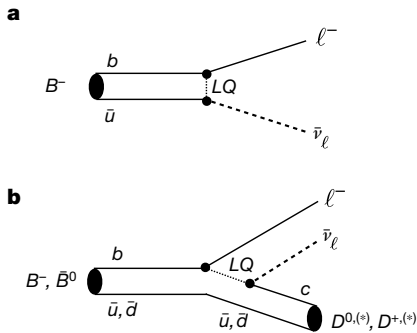


**Figure 7 | Diagrams for non-standard-model decay processes.**

**a**,  $B^- \rightarrow \ell^- \bar{\nu}_\ell$ , with a purely leptonic final state; **b**,  $B^- \rightarrow D^{(*)} \ell^- \bar{\nu}_\ell$ , involving a charm meson ( $D$  or  $D^*$ ) and lepton pair and mediated by a spin-0 leptoquark ( $LQ$ ).

distributions of the  $D^{(*)}$  and electron or muon<sup>33</sup> have been examined. Within the uncertainties of existing measurements, the observed shapes of these distributions are consistent with standard model predictions.

## Conclusions and outlook

Although the observed enhancements of the leptonic and semileptonic  $B$ -meson decay rates involving a  $\tau$  lepton relative to the expectations of the standard model of electroweak interactions are intriguing, their significance is not sufficient at present to establish a violation of lepton universality unambiguously. However, the fact that these unexpected enhancements have been observed by three experiments operating in very different environments deserves further attention.

At present, the measurements are limited by the size of the available data samples and uncertainties in the reconstruction efficiencies and background estimates. It is not inconceivable that the experiments have underestimated these uncertainties, or missed a more conventional explanation. Furthermore, although it is unlikely, it cannot be totally excluded that the theoretical standard model predictions are not as firm as assumed. The experimenters are continuing their analysis efforts, refining their methods, enhancing the signal samples by adding additional decay modes, improving the efficiency and selectivity of the tagging algorithms, as well as the Monte Carlo simulations, and scrutinizing all other aspects of the signal extraction.

In the near future, the LHCb collaboration will make several important contributions, among them their first measurement of the  $\bar{B} \rightarrow D\tau^-\bar{\nu}_\tau$  decay, which will also improve results for  $\bar{B} \rightarrow D^*\tau^-\bar{\nu}_\tau$ . Furthermore, the  $\tau^- \rightarrow \pi^-\pi^+\pi^-\bar{\nu}_\tau$  decay mode will be included. In addition, searches for lepton universality violation in semileptonic decays of other  $B$  mesons and baryons are being planned. Beyond that, LHCb will continue to record data at the highest  $pp$  collision energy available. By the end of 2017, the accumulated data sample is expected to increase by a factor of three. In the longer-term future, the LHCb collaboration is planning to further enhance the data rate capability and record much larger event samples.

At KEK in Japan, the  $e^+e^-$  collider is undergoing a major upgrade and is expected to enlarge the data sample by almost two orders of magnitude over a period of about ten years. In parallel, the capabilities of the Belle detector are also being upgraded. The operation of this new and more powerful detector is expected to start in 2018. The much larger event samples and the constrained  $B\bar{B}$  kinematics will allow more precise measurements of kinematic distributions and detailed studies of, for instance, the  $\tau$  polarization in  $B \rightarrow D^{(*)}\tau\nu_\tau$  decays. The feasibility of such a measurement was recently presented<sup>61</sup>. For  $B^- \rightarrow \tau^-\bar{\nu}_\tau$  decays, which currently have statistical and systematic uncertainties of 30% or more for individual measurements, the substantially larger data samples are expected to lead to major reductions in these uncertainties, allowing more accurate assessments of the compatibility with the standard model predictions. Detailed studies of the overall physics goals and precision measurements that can be achieved by the upgraded Belle and LHCb experiments are continuing.

In recent years, several experiments have examined decay rates and angular distributions for  $B^+$  decays involving a  $K^{(*)+}$  meson and a lepton pair,  $B^+ \rightarrow K^{(*)+}\mu^+\mu^-$  and  $B^+ \rightarrow K^{(*)+}e^+e^-$ . In the framework of the standard model these decays are very rare, since they involve  $b \rightarrow s$  quark transitions. The LHCb collaboration<sup>62</sup> recently published a measurement of the ratio:

$$\mathcal{R}_K = \frac{\mathcal{B}(B^+ \rightarrow K^+\mu^+\mu^-)}{\mathcal{B}(B^+ \rightarrow K^+e^+e^-)} = 0.745 \pm_{0.074}^{0.090} \pm 0.036 \quad (9)$$

This value is 2.6 standard deviations below the standard model expectation of about 1.0. Earlier measurements by the Belle<sup>63</sup>, CDF<sup>64</sup> and BaBar<sup>65</sup> collaborations had significantly larger uncertainties and were fully consistent with lepton universality. Some theoretical models include new types of interactions that can explain this result: for example, leptoquarks which can mediate this decay and result in higher rates for electrons than muons<sup>66,67</sup>. The BaBar<sup>65</sup>, LHCb<sup>68</sup> and Belle<sup>69</sup> collaborations have analysed angular distributions for the four decay modes and observed general agreement with standard model predictions, except for local deviations, the most significant by LHCb at the level of 3.4 standard deviations. More data are needed to enhance the significance of these measurements and find possible links to  $B$  decays involving  $\tau$  leptons.

If the currently observed excess in the ratios  $\mathcal{R}_D$  and  $\mathcal{R}_{D^*}$  is confirmed, experimenters will use their large data samples to measure properties of signal events and learn about the nature of the new particles and interactions that contribute to these decays<sup>70,71</sup>.

In conclusion, we can expect much larger event samples from the upgraded LHCb and Belle experiments in the not too distant future. These data will be critical to the effort to understand whether the tantalizing results obtained so far are an early indication of beyond-the-standard-model physics processes or the result of larger-than-expected statistical or systematic deviations. A confirmation of new-physics contributions in these decays would shake the foundations of our understanding of matter and trigger an intense programme of experimental and theoretical research.

**Received 15 December 2016; accepted 20 March 2017.**

- Mann, R. B. *An Introduction to Particle Physics and the Standard Model* (CRC, 2010).
- Weinberg, S. *The Quantum Theory of Fields. Vol. 2: Modern Applications* (Cambridge Univ. Press, 2013).
- Thomson, J. J. Carriers of negative electricity. In *Nobel Lectures: Physics, 1901–1921* (Elsevier, 1967).
- Neddermeyer, S. H. & Anderson, C. D. The nature of cosmic ray particles. *Phys. Rev.* **51**, 884–886 (1937).
- Perl, M. L. *et al.* Evidence for anomalous lepton production in  $e^+e^-$  annihilation. *Phys. Rev. Lett.* **35**, 1489–1492 (1975).
- Ablikim, M. *et al.* Precision measurement of the mass of the  $\tau$  lepton. *Phys. Rev. D* **90**, 012001 (2014).
- Lazzeroni, C. *et al.* Precision measurement of the ratio of the charged kaon leptonic decay rates. *Phys. Lett. B* **719**, 326–336 (2013).
- Pohl, R. *et al.* The size of the proton. *Nature* **466**, 213–216 (2010).
- Pohl, R., Gilman, R., Miller, G. A. & Pahuick, K. Muonic hydrogen and the proton radius puzzle. *Annu. Rev. Nucl. Part. Sci.* **63**, 175–204 (2013).
- Tanaka, M. Charged Higgs effects on exclusive semitauonic  $B$  decays. *Z. Phys. C* **67**, 321–326 (1995).
- Aoki, S. *et al.* Review of lattice results concerning low-energy particle physics. *Eur. Phys. J. C* **74**, 2890 (2014).
- Olive, K. A. *et al.* Review of particle physics. *Chin. Phys. C* **38**, 090001 (2014).
- Kobayashi, M. & Maskawa, T. CP violation in the renormalizable theory of weak interaction. *Prog. Theor. Phys.* **49**, 652–657 (1973).
- Amhis, Y. *et al.* Averages of  $b$ -hadron,  $c$ -hadron, and  $\tau$ -lepton properties. Preprint at <http://arxiv.org/abs/1412.7515> (2014).
- Charles, J. *et al.* CP violation and the CKM matrix: assessing the impact of the asymmetric  $B$  factories. *Eur. Phys. J. C* **41**, 1–131 (2005).
- Körner, J. G. & Schuler, G. A. Exclusive semileptonic heavy meson decays including lepton mass effects. *Z. Phys. C* **46**, 93–109 (1990).
- Na, H. *et al.*  $B \rightarrow D\ell\nu$  form factors at nonzero recoil and extraction of  $|V_{cb}|$ . *Phys. Rev. D* **92**, 054510 (2015); erratum **93**, 119906 (2016).
- Fajfer, S., Kamenik, J. F. & Nisandzic, I. On the  $B \rightarrow D^*\tau\bar{\nu}_\tau$  sensitivity to new physics. *Phys. Rev. D* **85**, 094025 (2012).
- Bailey, J. A. *et al.*  $B \rightarrow D\ell\nu$  form factors at nonzero recoil and  $|V_{cb}|$  from 2+1-flavor lattice QCD. *Phys. Rev. D* **92**, 034506 (2015).
- Aubert, B. *et al.* The BABAR detector. *Nucl. Instrum. Methods A* **479**, 1–116 (2002).

21. Aubert, B. *et al.* The BABAR detector: upgrades, operation and performance. *Nucl. Instrum. Methods A* **729**, 615–701 (2013).
22. Abashian, A. *et al.* The Belle detector. *Nucl. Instrum. Methods A* **479**, 117–232 (2002).
23. Alves, A. A. Jr *et al.* The LHCb detector at the LHC. *J. Instrum.* **3**, S08005 (2008).
24. Dettori, F. Performance of the LHCb detector during the LHC proton runs 2010–2012. *Nucl. Instrum. Methods A* **732**, 40–43 (2013).
25. Feindt, M. *et al.* A hierarchical neuroBayes-based algorithm for full reconstruction of  $B$  mesons at  $B$  factories. *Nucl. Instrum. Methods A* **654**, 432–440 (2011).
26. Lees, J. P. *et al.* Measurement of an excess of  $\bar{B} \rightarrow D^{(*)}\tau^{-}\bar{\nu}_{\tau}$  decays and implications for charged Higgs bosons. *Phys. Rev. D* **88**, 072012 (2013).  
**Detailed description of the measurement of  $\mathcal{R}_D$  and  $\mathcal{R}_{D^*}$  based on hadronic  $B$  tagging by BaBar and implication for potential interpretation in terms of two-Higgs doublet models.**
27. Kronenbitter, B. *et al.* Measurement of the branching fraction of  $B^{-} \rightarrow \tau^{+}\nu_{\tau}$  decays with the semileptonic tagging method. *Phys. Rev. D* **92**, 051102(R) (2015).  
**Currently the most precise measurement of  $B^{-} \rightarrow \tau^{-}\bar{\nu}_{\tau}$  decays by Belle based on semileptonic  $B$  tagging.**
28. Hara, K. *et al.* Evidence for  $B^{-} \rightarrow \tau^{-}\bar{\nu}_{\tau}$  with a hadronic tagging method using the full data sample of Belle. *Phys. Rev. Lett.* **110**, 131801 (2013).
29. Aubert, B. *et al.* A search for  $B^{+} \rightarrow \ell^{+}\nu_{\ell}$  recoiling against  $B^{-} \rightarrow D^{0}\ell^{-}\bar{\nu}X$ . *Phys. Rev. D* **81**, 051101 (2010).
30. Lees, J. P. *et al.* Evidence of  $B^{+} \rightarrow \tau^{+}\nu$  decays with hadronic  $B$  tags. *Phys. Rev. D* **88**, 031102 (2013).
31. Heavy Flavor Averaging Group. Compilation of  $B^{+}$  and  $B^0$  leptonic branching fractions. Available at [http://www.slac.stanford.edu/xorg/hfag/rare/ICHEP2016/radll/OUTPUT/HTML/radll\\_table4.html](http://www.slac.stanford.edu/xorg/hfag/rare/ICHEP2016/radll/OUTPUT/HTML/radll_table4.html) (October 2016).
32. Huschle, M. *et al.* Measurement of the branching ratio of  $\bar{B} \rightarrow D^{(*)}\tau^{-}\bar{\nu}_{\tau}$  relative to  $\bar{B} \rightarrow D^{(*)}\ell^{-}\bar{\nu}_{\ell}$  decays with hadronic tagging at Belle. *Phys. Rev. D* **92**, 072014 (2015).  
**Measurement of  $\mathcal{R}_D$  and  $\mathcal{R}_{D^*}$  with hadronic  $B$  tagging by Belle and studies of implications for two-Higgs doublet model type II.**
33. Sato, Y. *et al.* Measurement of the branching ratio of  $\bar{B}^0 \rightarrow D^{*+}\tau^{-}\bar{\nu}_{\tau}$  relative to  $\bar{B}^0 \rightarrow D^{*+}\ell^{-}\bar{\nu}_{\ell}$  decays with semileptonic tagging. *Phys. Rev. D* **94**, 072007 (2016).  
**Most recent measurement of  $\mathcal{R}_{D^*}$  by Belle based on semileptonic  $B$  tagging, placing constraints on possible new-physics scenarios.**
34. Aaij, R. *et al.* Measurement of the ratio of branching fractions  $\mathcal{B}(\bar{B}^0 \rightarrow D^{*+}\tau^{-}\bar{\nu}_{\tau})/\mathcal{B}(\bar{B}^0 \rightarrow D^{*+}\mu^{-}\bar{\nu}_{\mu})$ . *Phys. Rev. Lett.* **115**, 111803 (2015); addendum **115**, 159901 (2015).  
**First measurement of  $\mathcal{R}_{D^*}$  at  $pp$  collider by LHCb.**
35. Aubert, B. *et al.* Observation of the semileptonic decays  $B \rightarrow D^{*}\tau^{-}\bar{\nu}_{\tau}$  and evidence for  $B \rightarrow D\tau^{-}\bar{\nu}_{\tau}$ . *Phys. Rev. Lett.* **100**, 021801 (2008).
36. Aubert, B. *et al.* Measurement of the semileptonic decays  $B \rightarrow D\tau^{-}\bar{\nu}_{\tau}$  and  $B \rightarrow D^{*}\tau^{-}\bar{\nu}_{\tau}$ . *Phys. Rev. D* **79**, 092002 (2009).
37. Matyja, A. *et al.* Observation of  $B^0 \rightarrow D^{*+}\tau^{-}\bar{\nu}_{\tau}$  decay at Belle. *Phys. Rev. Lett.* **99**, 191807 (2007).
38. Bozek, A. *et al.* Observation of  $B^{+} \rightarrow \bar{D}^{*0}\tau^{+}\nu_{\tau}$  and evidence for  $B^{+} \rightarrow \bar{D}^{*0}\tau^{+}\nu_{\tau}$  at Belle. *Phys. Rev. D* **82**, 072005 (2010).
39. Heavy Flavor Averaging Group. Average of  $R_D$  and  $R_{D^*}$  for winter 2016. Available at [http://www.slac.stanford.edu/xorg/hfag/semi/winter16/winter16\\_dtaunu.html](http://www.slac.stanford.edu/xorg/hfag/semi/winter16/winter16_dtaunu.html) (March 2016).
40. Chatrchyan, S. *et al.* Search for a  $W'$  boson decaying to a bottom quark and a top quark in  $pp$  collisions at  $\sqrt{s}=7$  TeV. *Phys. Lett. B* **718**, 1229–1251 (2013).
41. Aad, G. *et al.* Search for  $W' \rightarrow tb$  in the lepton plus jets final state in proton-proton collisions at a centre-of-mass energy of  $\sqrt{s}=8$  TeV with the ATLAS detector. *Phys. Lett. B* **743**, 235–255 (2015).
42. Prieels, R. *et al.* Measurement of the parameter  $\xi''$  in polarized muon decay and implications on exotic couplings of the leptonic weak interaction. *Phys. Rev. D* **90**, 112003 (2014).
43. Stahl, A. *Physics with Tau Leptons* Vol. 160 of *Springer Tracts in Modern Physics* (Springer, 2000).
44. Chatrchyan, S. *et al.* Observation of a new boson at a mass of 125 GeV with the CMS experiment at the LHC. *Phys. Lett. B* **716**, 30–61 (2012).
45. Aad, G. *et al.* Observation of a new particle in the search for the standard model Higgs boson with the ATLAS detector at the LHC. *Phys. Lett. B* **716**, 1–29 (2012).
46. Barger, V. D., Hewett, J. L. & Phillips, R. J. N. New constraints on the charged Higgs sector in two-Higgs-doublet models. *Phys. Rev. D* **41**, 3421–3441 (1990).
47. Gunion, J. F. & Haber, H. E. Higgs bosons in supersymmetric models (I). *Nucl. Phys. B* **272**, 1–76 (1986); erratum **402**, 567 (1993).
48. Dorsner, I., Fajfer, S., Greljo, A., Kamenik, J. F. & Kosnik, N. Physics of leptoquarks in precision experiments and at particle colliders. *Phys. Rep.* **641**, 1–68 (2016).
49. Freytsis, M., Ligeti, Z. & Ruderman, J. T. Flavor models for  $\bar{B} \rightarrow D^{(*)}\tau\bar{\nu}$ . *Phys. Rev. D* **92**, 054018 (2015).
50. Datta, A., Duraisamy, M. & Ghosh, D. Diagnosing new physics in  $b \rightarrow c\tau\nu_{\tau}$  decays in the light of the recent BABAR result. *Phys. Rev. D* **86**, 034027 (2012).
51. Crivellin, A., Greub, C. & Kokulu, A. Explaining  $B \rightarrow D\tau\nu$ ,  $B \rightarrow D^{*}\tau\nu$  and  $B \rightarrow \tau\nu$  in a 2HDM of type III. *Phys. Rev. D* **86**, 054014 (2012).  
**Interpretation of  $\mathcal{R}_D$  and  $\mathcal{R}_{D^*}$  measurements in terms of a two-Higgs doublet model of type III.**
52. Fajfer, S., Kamenik, J. F., Nisandzic, I. & Zupan, J. Implications of lepton flavor universality violations in  $B$  decays. *Phys. Rev. Lett.* **109**, 161801 (2012).
53. Sakaki, Y., Tanaka, A., Tayduganov, M. & Watanabe, R. Testing leptoquark models in  $\bar{B} \rightarrow D^{(*)}\tau\bar{\nu}$ . *Phys. Rev. D* **88**, 094012 (2013).  
**Interpretation of  $\mathcal{R}_D$  and  $\mathcal{R}_{D^*}$  measurements in terms of leptoquark models.**
54. Dumont, B., Nishiwaki, K. & Watanabe, R. LHC constraints and prospects for  $S_1$  scalar leptoquark explaining the  $\bar{B} \rightarrow D^{(*)}\tau\bar{\nu}$  anomaly. *Phys. Rev. D* **94**, 034001 (2016).
55. Bauer, M. & Neubert, M. Minimal leptoquark explanation for the  $R_{D^{(*)}}$ ,  $R_K$ , and  $(g-2)_\mu$  anomalies. *Phys. Rev. Lett.* **116**, 141802 (2016).
56. Buchmüller, W., Rückl, R. & Wyler, D. Leptoquarks in lepton–quark collisions. *Phys. Lett. B* **191**, 442–448 (1987); erratum **448**, 320 (1999).
57. Chekanov, S. *et al.* A Search for resonance decays to lepton + jet at HERA and limits on leptoquarks. *Phys. Rev. D* **68**, 052004 (2003).
58. Aaron, F. D. *et al.* Search for first generation leptoquarks in  $ep$  collisions at HERA. *Phys. Lett. B* **704**, 388–396 (2011).
59. Aad, G. *et al.* Search for third generation scalar leptoquarks in  $pp$  collisions at  $\sqrt{s}=7$  TeV with the ATLAS detector. *J. High Energy Phys.* **6**, 33 (2013).
60. Khachatryan, V. *et al.* Search for pair production of third-generation scalar leptoquarks and top squarks in  $pp$  collisions at  $\sqrt{s}=8$  TeV. *Phys. Lett. B* **739**, 229–249 (2014).
61. Hirose, S. *et al.* Measurement of the  $\tau$  lepton polarization and  $R(D^*)$  in the decay  $\bar{B} \rightarrow D^{*}\tau^{-}\bar{\nu}_{\tau}$ . Preprint at <http://arxiv.org/abs/1612.00529> (2016).
62. Aaij, R. *et al.* Test of lepton universality using  $B^{+} \rightarrow K^{+}\ell^{+}\ell^{-}$  decays. *Phys. Rev. Lett.* **113**, 151601 (2014).
63. Wei, J. T. *et al.* Measurement of the differential branching fraction and forward-backward asymmetry for  $B^{+} \rightarrow K^{*0}\ell^{+}\ell^{-}$ . *Phys. Rev. Lett.* **103**, 171801 (2009).
64. Aaltonen, T. *et al.* Measurements of the angular distributions in the decays  $B \rightarrow K^{(*)}\mu^{+}\mu^{-}$  at CDF. *Phys. Rev. Lett.* **108**, 081807 (2012).
65. Lees, J. P. *et al.* Measurement of branching fractions and rate asymmetries in the rare decays  $B \rightarrow K^{(*)}\ell^{+}\ell^{-}$ . *Phys. Rev. D* **86**, 032012 (2012).
66. Hiller, G. & Schmaltz, M.  $R_K$  and future  $b \rightarrow s\ell\ell$  physics beyond the standard model opportunities. *Phys. Rev. D* **90**, 054014 (2014).
67. Bečrešić, D., Fajfer, S., Košnik, N. & Olcyr, S. Leptoquark model to explain the  $B$ -physics anomalies,  $R_K$  and  $R_D$ . *Phys. Rev. D* **94**, 115021 (2016).
68. Aaij, R. *et al.* Angular analysis of the  $B^0 \rightarrow K^{*0}\mu^{+}\mu^{-}$  decay using 3 fb $^{-1}$  of integrated luminosity. *J. High Energy Phys.* **2**, 104 (2016).
69. Wehle, S. *et al.* Lepton-flavor-dependent angular analysis of  $B \rightarrow K^{*}\ell^{+}\ell^{-}$ . Preprint at <http://arxiv.org/abs/1612.05014> (2016).
70. Sakaki, Y., Tanaka, M., Tayduganov, A. & Watanabe, R. Probing new physics with  $q^2$  distributions in  $\bar{B} \rightarrow D^{(*)}\tau\bar{\nu}$ . *Phys. Rev. D* **91**, 114028 (2015).
71. Alonzo, R., Kobach, A. & Martin Camalich, J. New physics in the kinematic distributions of  $\bar{B} \rightarrow D^{(*)}\tau^{-}(\rightarrow \ell^{-}\bar{\nu}_{\ell})\bar{\nu}_{\tau}$ . *Phys. Rev. D* **94**, 094021 (2016).

**Acknowledgements** We recognize the contributions and dedication of our colleagues in the large international collaborations supporting the operation of the BaBar (M.F.S., R.K., V.L.), Belle (T.K., Y.S.) and LHCb (G.C., B.H.) detectors, the data processing and the data analyses on which the results presented in this Review are based. None of this would have been achieved without the efforts of the teams at SLAC, KEK and CERN who achieved excellent beam conditions and delivered high luminosities of the  $e^{+}e^{-}$  and  $pp$  storage rings over many years. We acknowledge support from the Organisation for Scientific Research (NWO) of the Netherlands, the US National Science Foundation and Department of Energy, the Natural Sciences and Engineering Research Council (NSERC) of Canada, the Excellence Cluster of the DFG of Germany: Origin and Structure of the Universe, and the Japan Society for the Promotion of Science (JSPS).

**Author Contributions** All authors contributed to writing and editing the manuscript.

**Author Information** Reprints and permissions information is available at [www.nature.com/reprints](http://www.nature.com/reprints). The authors declare no competing financial interests. Readers are welcome to comment on the online version of the paper. Publisher's note: Springer Nature remains neutral with regard to jurisdictional claims in published maps and institutional affiliations. Correspondence and requests for materials should be addressed to V.L. ([luth@slac.stanford.edu](mailto:luth@slac.stanford.edu)).

**Reviewer Information** Nature thanks G. Isidori and the other anonymous reviewer(s) for their contribution to the peer review of this work.